Applied Catalysis A: General 491 (2015) 155–162

Contents lists available at ScienceDirect

Applied Catalysis A: General

journal homepage: www.elsevier.com/locate/apcata

Understanding the role of Co in Co–ZnO mixed oxide catalysts for the selective hydrogenolysis of glycerol

V. Rekha [a], C. Sumana [b,*], S. Paul Douglas [c], N. Lingaiah [a,*]

[a] Catalysis Laboratory, I&PC Division
[b] Chemical Engineering Division, CSIR-Indian Institute of Chemical Technology, Hyderabad 500 007, Telangana, India
[c] College of Engineering (A), Andhra University, Visakhapatnam 530 003, India

ARTICLE INFO

Article history:
Received 10 July 2014
Received in revised form 19 October 2014
Accepted 22 October 2014
Available online 30 October 2014

Keywords:
Glycerol
Cobalt oxide
Zinc oxide
Hydrogenolysis
1,2-Propanediol

ABSTRACT

A series of Co–ZnO catalysts with varying Co to Zn ratio were prepared by co-precipitation method and these were characterized by X-ray diffraction, temperature programmed reduction, H_2 chemisorption, X-ray photoelectron spectroscopy and transmission electron microscopy. The developed catalysts were evaluated for selective hydrogenolysis of glycerol to 1,2-propanediol. Glycerol conversion was found to be dependent on the ratio of Co to ZnO and a weight ratio Co/Zn of 50:50 was shown about 70% glycerol conversion with 80% selectivity to 1,2-propanediol. Glycerol hydrogenolysis activity was found to be related to Co metal area as well as amount of ZnO in the catalyst. The proposed catalysts were stable under the reaction conditions and reusable with consistent activity. Different reaction parameters were studied and optimum reaction conditions were established. A kinetic model for the hydrogenolysis reaction was also derived.

© 2014 Elsevier B.V. All rights reserved.

1. Introduction

Glycerol is a by-product in the preparation of biodiesel by transesterification of vegetable oils or animal fats is being produced in huge volumes and being accumulated worldwide with the expanding demand for biodiesel production [1]. The present demand for glycerol cannot compensate its production, and new efficient procedures for the transformation of glycerol to valuable chemicals are highly desired [2]. In future, glycerol will be a cost-effective raw material for the preparation of a wide range of valuable chemicals and fuel additives. Several routes are proposed for the conversion of glycerol to various value-added chemicals [3]. One of the methods for glycerol transformation is hydrogenolysis to 1,2-propanediol [4–6]. It is an attractive pathway as 1,2-propanediol is a major commodity chemical with a 4% annual market growth. 1,2-Propanediol is widely used in the preparation of several industrially important chemicals including unsaturated polyesters resins, functional fluids (antifreeze, de-icing, and heat transfer devices), pharmaceuticals, food, cosmetics, liquid detergents, tobacco humectants, flavors, fragrances, personal care, paints and animal feed [7–9]. Further there is increasing demand for 1,2-propanediol in antifreeze and deicing market due to the concern over toxicity of ethylene glycol based products to humans and animals.

Acid or base catalysts are effective for the dehydration of alcohols, whereas metals are effective for hydrogenation. For hydrogenolysis of glycerol, metal–acid/base bifunctional catalysts have been studied [8]. A variety of heterogeneous catalysts have been tested for this reaction which can be classified mainly into two groups. The first type of catalysts are based on noble metals such as Rh, Ru, Pd, Ir, Re and Pt [10–15] and other type of catalysts are non-noble metals such as Cu, Co and Ni [16–20]. The Cu based catalysts are highly selective toward 1,2-propanediol as compared to noble metal catalysts due to its lower activity for C—C bond cleavage. However, sintering of metal particles during the course of reaction often resulted in catalyst deactivation. Also it is reported that the conversion and selectivity of glycerol is effected by the acidic [6,21,22] and basic promoters [23,24]. Comparison of different catalysts under neutral [4], acidic [6] and basic conditions [7] have been reported in the literature. Guo et al. studied glycerol hydrogenolysis using Co supported on MgO catalysts resulting 44.8% glycerol conversion and 42.2% selectivity toward 1,2-propanediol [25]. Recently, Balaraju et al. reported Cu/MgO catalysts for hydrogenolysis of glycerol with improved selectivity toward 1,2-propanediol [26]. However, with these catalysts the glycerol conversion was found to be low and the problems such as conversion of support MgO to $Mg(OH)_2$ and aggregation of cobalt particles occurred during the reaction. Therefore, in order to

* Corresponding authors. Tel.: +91 40 27191722; fax: +91 40 27160921.
E-mail addresses: sumana@iict.res.in (C. Sumana), nakkalingaiah@iict.res.in (N. Lingaiah).

http://dx.doi.org/10.1016/j.apcata.2014.10.042
0926-860X/© 2014 Elsevier B.V. All rights reserved.

overcome the above drawbacks, improved catalysts consisting of Co supported on ZnO are proposed for the selective hydrogenolysis of glycerol to 1,2-propanediol.

In the present work, a series of Co–ZnO catalysts were prepared with varying Co/Zn weight ratios and studied for selective hydrogenolysis of glycerol. These catalysts were characterized by employing different spectroscopic methods. The derived physicochemical properties were correlated with the observed glycerol hydrogenolysis activity. Further, the process conditions were optimized to improve the conversion and selectivity. Finally a kinetic model was proposed for the glycerol hydrogenolysis.

2. Experimental

2.1. Catalyst preparation

Co–ZnO catalysts with varying Co/ZnO weight ratio were prepared using co-precipitation method. Calculated amounts of aqueous solutions of $Co(NO_3)_2{\cdot}6H_2O$ and $Zn(NO_3)_2{\cdot}6H_2O$ were taken and 0.5 M solution of potassium carbonate was added drop wise with constant stirring until the pH of the solution becomes 10. The formed precipitate was kept on stirring for a period of 12 h. The formed solid was collected by filtration and washed thoroughly with water to remove any traces of potassium. The sample was then dried in oven for overnight at 100 °C. The dried samples were calcinated in air at 400 °C for 3 h to obtain final catalyst. Different catalyst compositions were prepared by varying the amount of Co in Co–ZnO from 20 to 70 wt%.

2.2. Catalyst characterization

The surface area of the samples was measured by N_2-physisorption at −196 °C using Micromeritics ASAP 2000. Approximately 0.2 g of sample was used for each analysis. The moisture and other adsorbed gases present in the sample were removed before analysis by degassing the sample at 200 °C.

X-ray powder diffraction (XRD) patterns of the catalysts were recorded on a Rigaku Miniflex X-ray diffractometer using Ni filtered Cu Kα radiation (λ = 1.5406 Å) with a scan speed of 2° min^{-1} and a scan range of 10–80° at 30 kV and 15 mA.

Hydrogen chemisorption was carried out on a pulse adsorption apparatus. Prior to adsorption measurements each catalyst sample (100 mg) was reduced in a flow of hydrogen (50 ml/min) at 450 °C for 2 h and flushed subsequently in pure Ar flow and cooled to 150 °C in the same gas flow. H_2 uptake was measured by injecting number of H_2 pulses through a calibrated on-line sampling valve. H_2 pulses were injected until there was no more adsorption by catalyst. The metal surface area and particle size of the catalysts were calculated assuming the stoichiometric factor for hydrogen atom to Co as 1.

Temperature programmed reduction (TPR) of the catalysts was carried out in a flow of 5% H_2/Ar mixture gas at a flow rate of 60 ml/min with a temperature ramp of 10 °C/min. Before TPR run the catalysts were pretreated in Ar at 300 °C for 2 h. The hydrogen consumption was monitored using a thermal conductivity detector.

X-ray photo electronic spectroscopy (XPS) measurements were conducted on a KRATOS AXIS 165 with a DUAL anode (Mg and Al) apparatus using Al K_α anode. The non-monochromatized Al-K_α X–ray source ($h\nu$ = 1486.6 eV) was operated at 12.5 kV and 16 mA. Before acquisition of data the sample was out-gassed for about 3 h at 100 °C under vacuum of 1.0×10^{-7} Torr to minimize surface contamination. The XPS instrument was calibrated using Au as standard. For energy calibration, the carbon 1*s* photoelectron line was used and the carbon 1*s* binding energy was taken as 285 eV. Charge neutralization of 2 eV was used to balance the charge up of the sample. The spectra were deconvoluted using Sun Solaris based Vision-2 curve resolver. The location and the full width at half maximum (FWHM) value for the species were first determined using the spectrum of pure sample. Symmetric Gaussian shapes were used in all cases. Binding energies for identical samples were, in general, reproducible within ±0.1 eV.

The morphology features of the catalysts were obtained by transmission electron microscopy (TEM). TEM investigations were carried out using Philips CM20 (100 kV) transmission electron microscope equipped with a NARON energy-dispersive spectrometer with a germanium detector. The specimens were prepared by dispersing the samples in methanol using an ultrasonic bath and evaporating a drop of resultant suspension onto the lacey carbon support grid. The sizes of the catalyst particles were measured by digital micrograph software (version 3.6.5, Gatan Inc.).

Semi-quantitative chemical analyses on grains were carried out using Hitachi S-3400N Scanning Electron Microscope coupled with Energy Dispersive Spectrometer (SEM-EDS). Horiba EDS detector was used for the analysis with operating conditions: accelerating voltage of 15 kV beam current of 2.9 nA and measurement time 60 s. Atomic ratios were calculated with the ZAF-4® program, which performs the necessary corrections for the overlapping peaks of different elements.

2.3. Glycerol hydrogenolysis activity measurements

Hydrogenolysis of glycerol was carried out in 100-mL Hastealloy PARR 4843 autoclave. Prior to the experiment, the Co–ZnO catalyst was reduced at 450 °C for 2 h with a hydrogen flow of 60 ml/min. In a typical run, 20 g of the aqueous glycerol solution (20 wt% glycerol) and 0.6 g of catalyst were loaded into the reactor. The autoclave was purged with H_2 flow to drive off the air present in it. The glycerol hydrogenolysis reaction was conducted at a temperature of 180 °C with a H_2 pressure of 40 bar at a rotation speed of 300 rpm. During the reaction, hydrogen pressure was noticed to be decreased and it was maintained by introducing additional H_2.

2.4. Analysis of glycerol hydrogenolysis products

After completion of the reaction, gaseous products were collected in a gasbag and the liquid phase products were separated from the catalyst by filtration. The liquid products were analyzed using a gas chromatograph (Shimadzu 2010) equipped with a flame ionization detector by separating them on Inno wax capillary column (diameter 0.25 mm, length 30 m). The products were identified by using GC–MS (Shimadzu, GCMS-QP2010S) analysis. The gas phase products were analyzed by a gas chromatograph equipped with Porapak Q column and thermal conductivity detector. The products identified during glycerol hydrogenolysis were 1,2-propanediol and ethylene glycol (EG) as main products and 1-propanol, 2-propanol, ethanol, methanol, ethane and methane as degradation products. Following are the equations used for evaluating the conversion and selectivity of glycerol to 1,2-propanediol.

$$\text{Conversion}\ (\%) = \frac{\text{moles of glycerol consumed}}{\text{moles of glycerol intitially charged}} \times 100.$$

$$\text{Selectivity}\ (\%) = \frac{\text{moles of carbon in specific product}}{\text{moles of carbon in all detected product}} \times 100.$$

Table 1
Physico-chemical properties of Co–ZnO catalysts.

Catalyst composition Co:ZnO (wt%)	BET surface area[a] (m^2/g)	Specific metal area[b] (m^2/g)	Particle size[b] (nm)
20:80	49.9	0.7	18.2
30:70	47.6	1.1	19.8
40:60	35.4	1.2	20.0
50:50	32.9	1.6	20.9
60:40	30.9	1.4	29.3
70:30	29.5	1.4	33.9

[a] BET surface area determined from N_2 gas absorption.
[b] Co metal surface area and particle size obtained from H_2 pulse chemisorption.

3. Results and discussion

3.1. Physico-chemical properties of the catalysts

The physico-chemical properties of the catalysts were reported in Table 1. Surface area of the catalysts was found to be decreased with the increase in cobalt content in the Co–ZnO catalysts. The decrease in BET surface area can be attributed to the occupation of Co particles on the surface of ZnO. The metal surface area of the catalysts was found to exhibit an increasing trend with the increase in weight ratio of Co to ZnO and attained maximum for the catalyst with a ratio of 50:50. The increment in Co metal surface area with the increase in Co loading on ZnO support had ensured the uniform distribution of Co metal particles. However, the metal surface area of Co was found to be decreased for the catalysts with Co content more than 50 wt%. The decrease in Co surface area was mainly due to the formation of large crystallites at high Co content on the ZnO. The particle size of catalysts was more or less similar up to 50 wt% of Co loading. The marginal increment in the surface of Co metal particles with the increase in Co metal loading reveals the fact that the textural parameters of ZnO were well preserved in the Co–ZnO catalysts. Alternatively it can be understood that the Co metal particles were well distributed on ZnO.

The XRD patterns of the calcined and reduced Co–ZnO samples are shown in Fig. 1(A) and (B) respectively. The patterns suggest the presence of well crystalline phases of Co and ZnO. XRD patters related to ZnO were predominant for the samples with low Co content. The peaks at 31.6°, 34.4°, 36.0°, 47.6°, 56.5°, 62.8°, 67.9° and 69.0° correspond to 100, 002, 101, 102, 110, 103, 112, and 201 reflection planes of hexagonal close packed wurtzite structure of ZnO respectively. The catalysts with high Co content (>40%) were found to exhibit crystallite sites related to the crystal planes of cubic Co_3O_4 (PDF#42-1467). The formation of mixed oxide phase $ZnCo_2O_4$ was not ruled out at certain composition of these oxides. The patterns of both Co_3O_4 and $ZnCo_2O_4$ are not distinguishable by XRD. From Fig. 1(A) the presence of ZnO phase in the catalysts was found to be decreased with the increase in Co loading ensuring the possible formation of mixed oxide phase.

The catalysts were reduced at 450 °C before they were used for glycerol hydrogenolysis. The XRD patterns of the reduced catalysts, as shown in Fig. 1(B) suggest that the crystalline nature of the catalysts was decreased with increase in Co content in the catalyst after reduction. The Co_3O_4 phase present in freshly prepared catalysts disappeared after reduction suggesting that it was reduced to either CoO or Co metal particles [27]. The absence of patterns related to CoO or Co metal reveals the formation of nanosize CoO or Co particles during the reduction.

In order to investigate the reducibility of Co oxides in the Co–ZnO catalysts, TPR analysis was conducted, and the corresponding profiles are shown in Fig. 2. Two main distinct reduction peaks were observed, one at low temperature and another at relatively high temperature. The low temperature peak can be ascribed to the reduction of Co_3O_4 to CoO and high temperature peak can be related to the reduction of CoO to metallic Co. A distinct shift was noticed in both the reduction peak maxima to higher temperature with increase in Co content up to 60 wt%. Similar observations were also reported elsewhere for cobalt catalysts [28,29]. The catalysts with high Co content (80 wt%) were shown similar reduction temperatures as that of bulk Co_3O_4. The shift in the reduction temperature with Co loading can be mainly related to the reduction of mixed oxide phases that were formed at moderate Co content of about 50 wt%. Under these compositions the formation of $ZnCo_2O_4$ phase was quite possible and it can get reduced in two steps i.e. $ZnCo_2O_4$ to CoO followed by CoO to Co [30–32]. The absence of ZnO phase in XRD beyond the 60% of Co also supports the formation of $ZnCo_2O_4$ phase and supplements the observations made from TPR.

X-ray photoelectron spectra of Co–ZnO catalyst after reduction are shown in Fig. 3. The Co 2*p* spectrum of Co–ZnO (50:50) shows two broad and asymmetric peaks separated by a spin orbit splitting of 15 eV. The B.E for $Co2p_{3/2}$ and $Co2p_{1/2}$ were observed at 780.19 and 795.12 eV respectively, along with two satellite peaks at 787.7

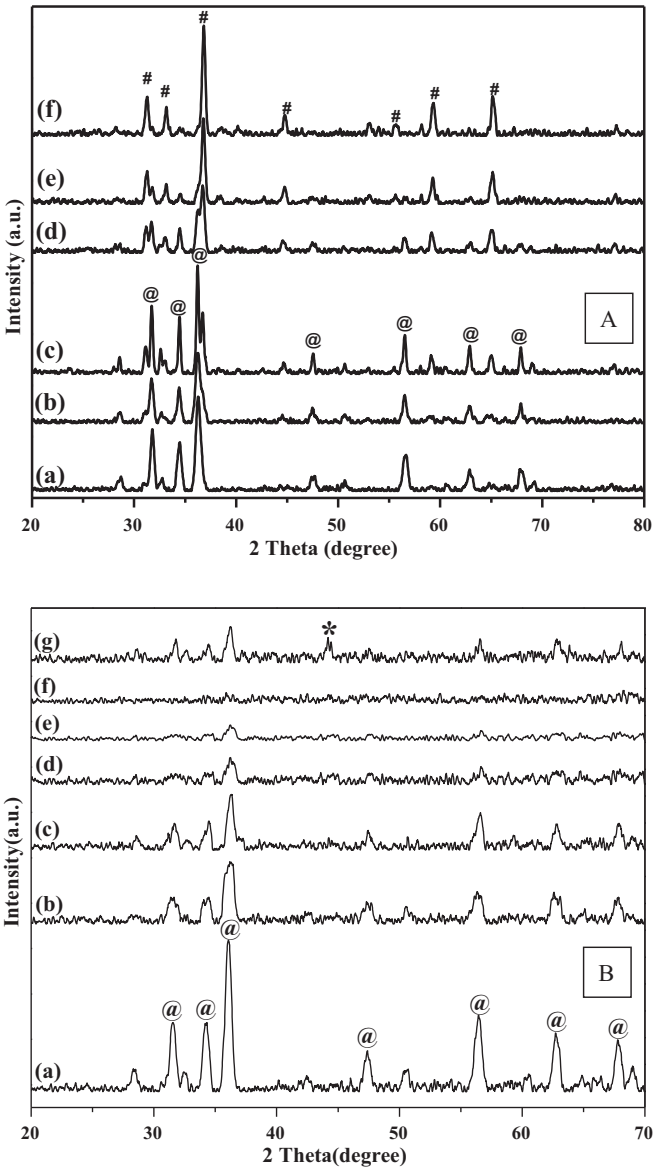

Fig. 1. X-ray diffraction patterns of (A) calcined (B) reduced and used Co–ZnO catalysts. (a) 20:80 Co–ZnO, (b) 30:70 Co–ZnO, (c) 40:60 Co–ZnO, (d) 50:50 Co–ZnO, (e) 60:40 Co–ZnO, (f) 70:30 Co–ZnO, (g) 50:50 Co–ZnO used; (@) ZnO, (#) Co_3O_4, (*) Co phases.

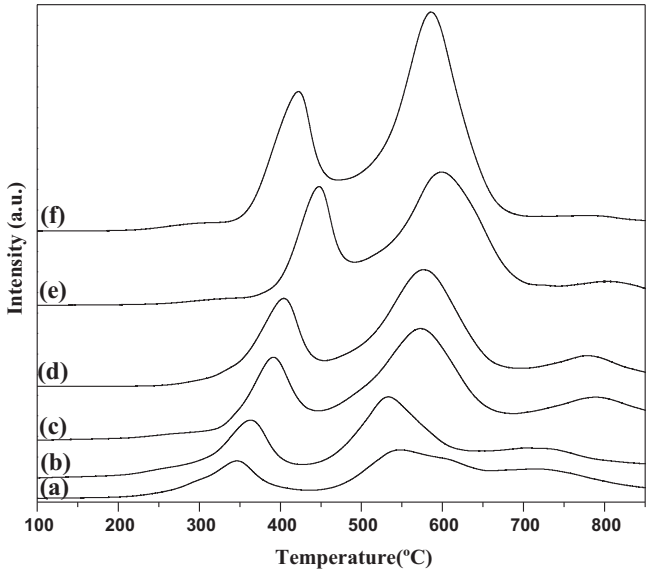

Fig. 2. Temperature programmed reduction profiles of Co–ZnO catalysts. (a) 20:80 Co–ZnO, (b) 30:70 Co–ZnO, (c) 40:60 Co–ZnO, (d) 50:50 Co–ZnO, (e) 60:40 Co–ZnO, (f) 70:30 Co–ZnO.

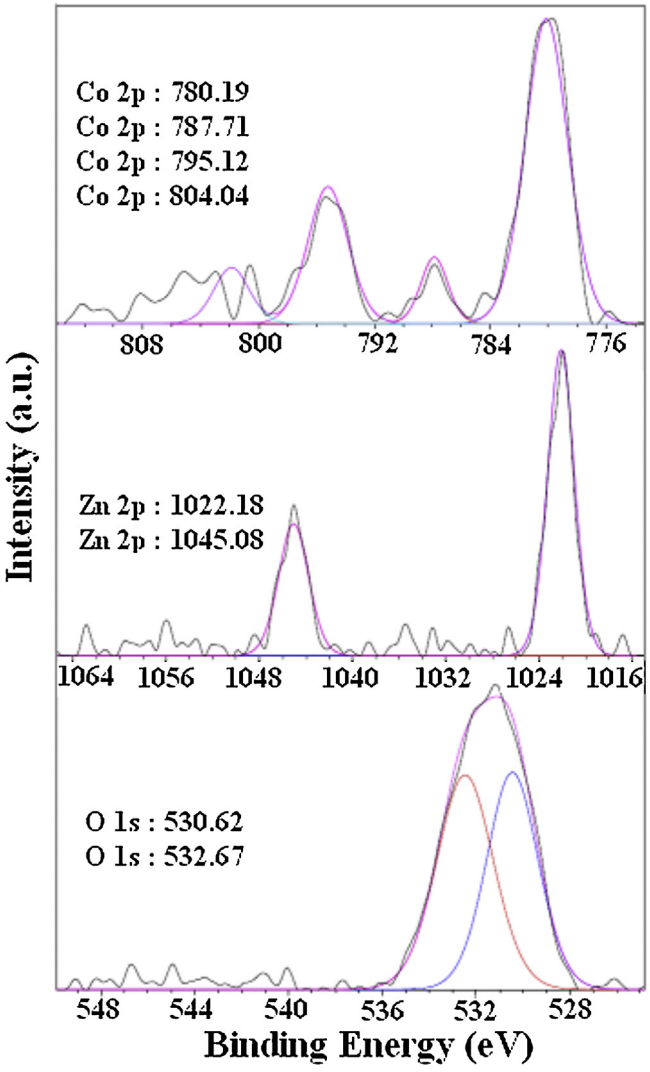

Fig. 3. X-ray photoelectron spectroscopy profiles of 50:50 Co–ZnO catalyst.

and 804.0 eV. A weak satellite located about 7 eV above the main peak, shown by the Co2$p_{3/2}$ spin orbital, suggests the presence of Co^{2+} species. The presence of satellite peak at 787.7 eV was related to CoO and these satellite peaks were typical for Co ions in the divalent Co^{2+} state and they were not observed for Co^{3+}. The binding energies of the Zn2p3/2 and Zn2p1/2 peaks are observed at 1022.18 and 1045.08 eV respectively, which ensures the presence of Zn^{2+} ions. The O1s surface XPS peak at 530.6 eV referred to the cobalt oxide, showed a shoulder at 532.6 eV attributed to the presence of hydroxyl species or adsorbed water on the surface, which are commonly observed in air exposed samples. From XPS studies of reduced catalyst it is noted that the surface cobalt was oxidized. This may be due to the re-oxidization of catalyst metal surface occurred during its brief exposition to air between the reduction and XPS analysis tests.

TEM images of the Co–ZnO (50:50) catalyst before and after the reaction were shown in Fig. 4. The dark zones in the images correspond to Co particles, whereas the lighter zones signify the presence of ZnO. The dark metallic Co particles were found to be dispersed on the platelet like ZnO. The average particle size of these particles was estimated by considering the minimum and maximum diameter of large number of particles. The average particle size was found to be in the range of 20–25 nm. TEM images ensure that similar morphology was maintained during the hydrogenolysis of glycerol and also suggest that there was no indication of any agglomeration during the reaction.

The Co–ZnO catalysts were inspected by scanning electron microscopy (SEM) with EDX in order to analyze both the morphological and chemical characteristics. The EDX analysis of Co–ZnO (50:50) catalyst reveals that Co and Zn were present with 35.3 and 15.6 at.% respectively.

3.2. Glycerol hydrogenolysis activity measurements

3.2.1. Effect of Co content in ZnO on glycerol hydrogenolysis

Hydrogenolysis of glycerol reaction was studied over Co–ZnO catalysts and the results are presented in Fig. 5. The results suggested that with increase in the Co to ZnO weight ratio, the glycerol conversion was found to be increased and attained a maximum for the catalyst with a ratio of 50:50. The maximum activity achieved with this catalyst was about 70% glycerol conversion with 80% selectivity toward 1,2-propanediol. The conversion of glycerol achieved with the catalysts of this work, is much better than the conversion attained by the previously reported Co based catalysts such as Co/MgO [26,27]. ZnO effectively catalyzes the dehydration of glycerol into acetol and Co does the hydrogenation of acetol into 1,2-propanediol. Similar observation was noted with Cu/ZnO catalysts [33]. The high activity of Co–ZnO catalysts can be explained based on their physico chemical properties. In general, the catalysts after reduction mainly contain CoO and Co metal species and during the course of the reaction CoO may reduced to Co particles. The used catalyst was subjected to XRD analysis and the patterns are shown in Fig. 1B (g). A small diffraction peak related to Co particles was observed. This indicates that some CoO might be reduced to Co metal. One cannot exclude the possibility of increase in Co particle size during the reaction. Guo et al. [27] observed the XRD patterns related to Co after glycerol hydrogenolysis indicating that CoO present in the catalyst reduced to Co. In our case also weak diffraction peaks related to Co was observed. The SEM EDX analysis also suggests the presence of more number of Co particles on the surface of the Co–ZnO (50:50) catalyst. The presence of well-dispersed nanosize Co metal particles might be responsible for the high activity of the catalyst. In order to understand the role of Co metal particles, the relation between glycerol conversion and Co metal area was plotted and shown in Fig. 6. This figure suggests a linear relationship between Co metal area and hydrogenolysis

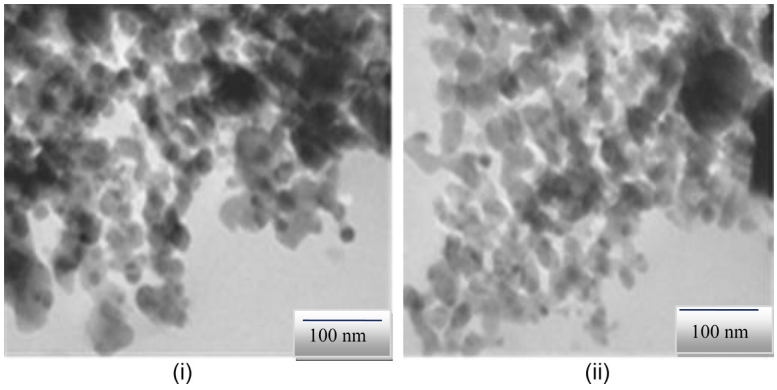

Fig. 4. TEM micrographs of 50:50 Co–ZnO catalyst. (i) Fresh and (ii) used.

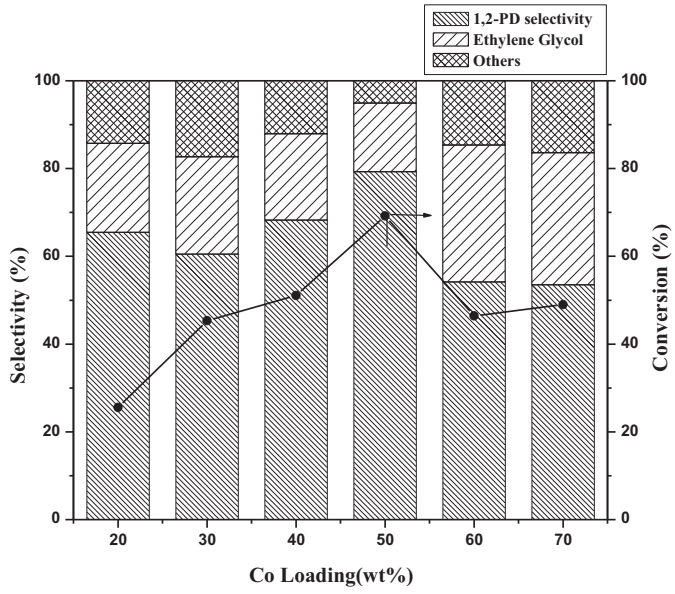

Fig. 5. Effect of Co to Zn ratio in Co–ZnO catalysts on glycerol hydrogenolysis. Reaction conditions: 50 ml of 20 wt% glycerol aqueous solution; H_2 pressure: 40 bar; reaction time: 8 h; catalyst weight: 600 mg; reaction temperature: 180 °C.

activity. The maximum conversion of glycerol is achieved with the 50 wt% Co/ZnO catalyst which is exhibiting maximum metal area as depicted from Table 1. Further, a decreasing trend in glycerol conversion is observed with the increase in Co loading which can be mainly due to the agglomerisation of the Co particles. It is to be noted from the results of Table 1 that the surface area of the catalysts is decreased with the increase in Co loading. These results suggest that the catalyst with high metal surface area demonstrated high glycerol hydrogenolysis activity. Thus, The Co–ZnO (50:50) catalyst is considered for further study.

3.2.2. *Influence of reaction temperature*

The influence of reaction temperature on glycerol hydrogenolysis to 1,2-propanediol was studied in the range of 160–220 °C over 0.6 g of Co–ZnO (50:50) catalyst at 40 bar H_2 with a reaction time of 8 h. Fig. 7 shows the effect of reaction temperature on conversion and selectivity in glycerol hydrogenolysis. The glycerol conversion rate is found to be increased with the increase in reaction temperature from 160 to 180 °C, further increase in temperature could improve the reaction rate marginally up to 220 °C. However, the selectivity of glycerol to 1,2-propanediol was found to be decreased with the increase of temperature. This behavior can be anticipated to the fact that C—C bond hydrogenolysis of 1,2-propanediol to ethylene glycol and other lower alcohols occurred on Co sites of the catalyst at high temperatures. The temperature of 180 °C is considered for further study.

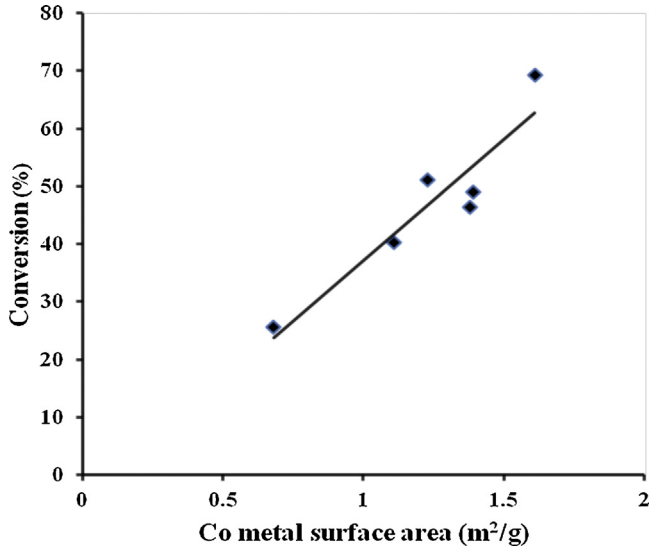

Fig. 6. Correlation between Co metal area and glycerol conversion.

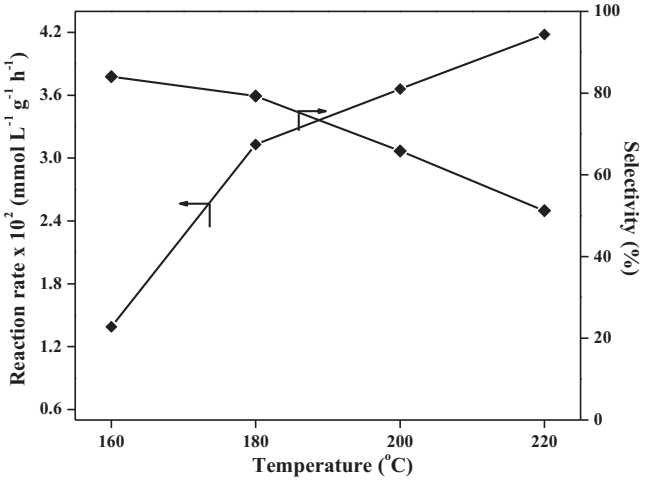

Fig. 7. Influence of reaction temperature on glycerol hydrogenolysis over Co–ZnO catalyst. Reaction conditions: 50 ml of 20 wt% glycerol aqueous solution; H_2 pressure: 40 bar; reaction time: 8 h; catalyst weight: 600 mg.

Table 2
Comparison of various Co based catalysts with the proposed Co–ZnO catalyst for glycerol hydrogenolysis.

Catalyst	Reaction conditions	Conversion (%)	Selectivity (%)	Reference
Co–MgO	Temp.: 200 °C H_2 pressure: 20 bar Glycerol conc.: 10 wt% Catalyst weight: 0.2 g Time: 9 h	44.8	42.2	[26]
Co–Zn–Al	Temp.: 200 °C H_2 pressure: 20 bar Glycerol conc.: 10 wt% Catalyst weight: 0.3 g Time: 12 h	67.7	50.5	[27]
Cu–ZnO	Temp.: 200 °C H_2 pressure: 20 bar Glycerol conc.: 20 wt% Catalyst weight: 1.2 g Time: 16 h	37	92.0	[33]
Hierarchical Co micro/nanocomposites	Temp.: 220 °C H_2 pressure: 60 bar Glycerol conc.: 5 wt% Catalyst weight: 0.1 g Time: 8 h	25.8	60.2	[35]
Co–ZnO	Temp.: 180 °C H_2 pressure: 40 bar Glycerol conc.: 20 wt% Catalyst weight: 0.6 g Time: 8 h	70.0	80.0	Present study

3.2.3. Effect of reaction time

The effect of reaction time on the glycerol conversion and selectivity to 1,2-propanediol was studied. This effect is studied by keeping the reaction temperature as 180 °C at 40 bar H_2 pressure over 0.6 g of Co–ZnO (50:50) catalyst. Within 4 h duration of reaction time, about 43% of glycerol conversion was achieved with 69% selectivity toward 1,2-propanediol. Further, within 8 h of reaction time the present catalyst gave about 70% conversion of glycerol. This reaction time is much less as compared to most of the reported catalysts [5,34]. It is important to highlight that the present catalyst was selective in forming more than 60% 1,2-propanediol irrespective of the reaction time.

3.2.4. Effect of hydrogen pressure

Reactions were carried out at different hydrogen pressures varying from 20 to 60 bar over 0.6 g of Co–ZnO (50:50) catalyst at a constant reaction temperature of 180 °C and reaction time of 8 h. With the increase in H_2 pressure from 20 to 40 bar, the rate of glycerol conversion is increased from 2.077 to 3.134×10^2 mmol L^{-1} g^{-1} h^{-1}. At the same time the selectivity to 1,2-propanediol was found to be increased from 66 to 79%. Further increase in H_2 pressure up to 60 bar resulted a decrease in the glycerol activity which can be due to the degradation of formed 1,2-propanediol to ethylene glycol or other lower alcohols at high pressures. Therefore the pressure of 40 bar is considered to be optimum.

3.2.5. Effect of glycerol concentration

In order to achieve maximum productivity of 1,2-propanediol, the effect of glycerol concentration on the conversion rate was studied in the range of 10–40 wt% of glycerol concentration under the reaction conditions of 180 °C, 40 bar H_2 and 8 h with 0.6 g of 50:50 Co–ZnO catalyst. Glycerol hydrogenolysis rate was increased with the increase in glycerol concentration from 10 to 40 wt%. It was observed that, the conversion rate of glycerol was decreased with the increase in initial glycerol concentration. This can be due to the inadequate number of catalyst active sites for the increased number of glycerol molecules to react, as the quantity of catalyst was maintained constant. The selectivity to 1,2-propanediol was 80% at 20 wt% glycerol and it was almost remained same for further increase in glycerol concentration up to 40 wt%. The decrease in selectivity was observed at low glycerol concentration, which can be due to the cleavage of C—C bond of 1,2-propanediol, as the availability of glycerol was not sufficient.

3.2.6. Reusability of the catalyst

Experimental studies were performed to explore the recyclability of the catalyst. In order to establish the reusability of catalyst for glycerol hydrogenolysis, after using for first reaction, the catalyst was filtered, washed with methanol and reused for the next subsequent run. It was observed about 68.7% conversion after the third recycle. A marginal variation of less than 2% in the overall conversion of glycerol was noticed after three cycles. The used catalyst was characterized by XRD and TEM. The comparison of TEM images of fresh catalyst samples with used ones as in Fig. 4, suggest that there was no indication of agglomeration during glycerol hydrogenolysis. These results demonstrate that the Co–ZnO catalyst for glycerol hydrogenolysis is reusable with consistent activity and found to be stable under present experimental conditions.

3.2.7. Comparison of Co–ZnO catalysts with other reported Co based catalysts.

Table 2 compares the performance of the Co–ZnO catalyst with the other Co-based catalysts reported in literature for the hydrogenolysis of glycerol. The present catalyst was exhibited high selectivity as compared to other Co based catalysts such as Co–MgO and Co–Zn–Al [26,32]. Though the Cu–ZnO catalyst exhibited high selectivity, the overall conversion of glycerol was low as compared to the present catalyst [33]. More importantly, the present catalyst was resulted optimum activity in short reaction time as compared to the reported catalysts.

3.3. Kinetic studies

The liquid phase glycerol hydrogenolysis in the presence of Co–ZnO catalyst forms a typical example for gas–liquid–solid reaction system. For such systems, unless the absence of mass and heat transfer resistances is ensured, true models representing the reaction kinetics cannot be directly developed using experimental data. For the present reaction, the gas phase mass transfer

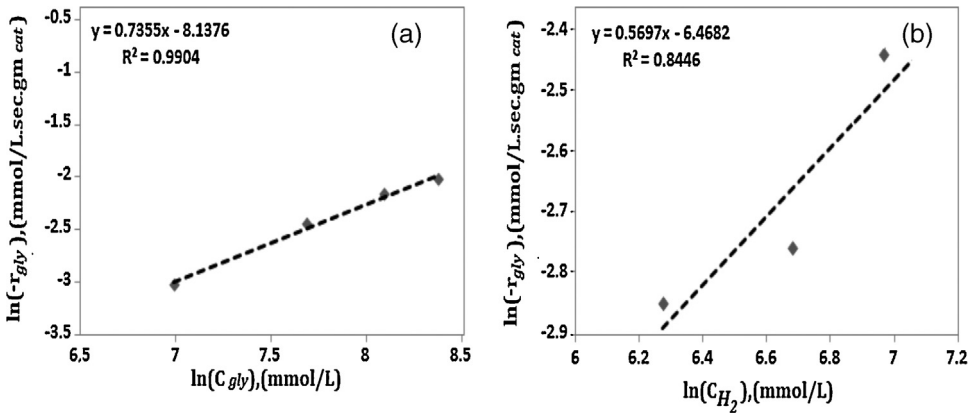

Fig. 8. Glycerol consumption rate: (a) apparent reaction order with respect to glycerol and (b) apparent reaction order with respect to hydrogen.

resistance can be considered to be negligible as the gas phase in the reactor consists of mainly H_2 and gas–liquid inter phase is instantaneously saturated with H_2. Further, the liquid phase mass transfer resistance can be considered to be negligible ensuring the uniform mixing of reactants. A stirrer speed of 500 rpm is considered in the present study as suggested from previous literature reported on similar systems. It was also ensured that, there exists no significant change in initial reaction rate with further increase or decrease in stirrer speed. Moreover, it was observed a linear relation between the catalyst weight and rate of reaction justifying the absence of external mass transfer resistances. In addition, the internal pore diffusion resistances can also be treated as negligible, as the catalyst considered in this study was in uniform powdered form. Further, heat transfer resistances were also considered to be insignificant ensuring the absence of temperature gradients within the reactor. Therefore, it can be stated that, the actual kinetics of liquid phase glycerol hydrogenolysis in the presence of Co–ZnO catalyst can be obtained through proper experimentation.

The reaction kinetics was studied by conducting experiments at varied reaction parameters such as temperature, H_2 pressure, and glycerol concentration. The kinetic parameters were calculated based on the total glycerol consumption and the resulted experimental data is fitted to a simple power law model. Thus, the rate expression characterizing the glycerol hydrogenolysis reaction can be given as,

$$(-r_{\mathrm{gly}}) = -\frac{d(\mathrm{C_{gly}})}{dt} = k(\mathrm{C_{gly}})^m(\mathrm{C_{H_2}})^n \quad \text{(A1)}$$

where k is the rate constant, m and n represent the reaction orders with respect to glycerol and hydrogen respectively. Such expression was considered elsewhere for representing the kinetics of glycerol hydrogenolysis reaction with other catalysts [36,37]. The experimental data resulted by conducting the reactions with varied glycerol concentration from 10 to 40 wt% while maintaining all the other parameters constant at their optimal values was considered for evaluating the reaction order with respect to glycerol. Similarly, the reaction order with respect to hydrogen was evaluated by considering the experimental data concerned to the reactions conducted by varying hydrogen pressure from 20 to 40 bar while maintaining all the other parameters constant at their optimal values. The glycerol consumption rate was plotted w.r.t. the concentrations of reactants glycerol and hydrogen respectively in figures Fig. 8(a) and (b). It is noted from figure that, the increase in concentrations of both the reactants glycerol and hydrogen tends to improve the glycerol conversion rate. The hydrogenolysis of glycerol in the presence of Co–ZnO catalyst, the apparent reaction order resulted with respect to glycerol was 0.7355 and that with respect to hydrogen was 0.5697. These values ensure that the rate of glycerol hydrogenolysis is dependent on the glycerol concentration to the larger extent as compared to that of hydrogen concentration.

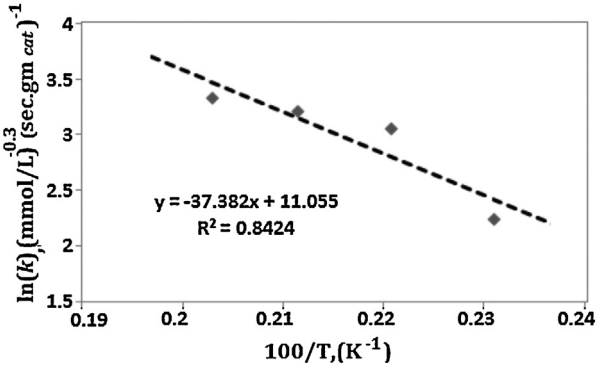

Fig. 9. Arrhenius plot for overall reaction of glycerol hydrogenolysis.

The temperature dependency of the rate constant k is given by the Arrhenius equation defining as,

$$k = k_o e^{-(E/RT)} \quad \text{(B1)}$$

where k_o and E are the Arrhenius constants, R is the universal gas constant and T is the temperature. The reactions were conducted at different temperatures in the range of 160–220 °C and the corresponding rate constants were evaluated by using equation Eq. (A1). The Arrhenius law plotted $\ln(k)$ vs. $1/T$ was resulted in a straight line as given in Fig. 9. The values of activation energy and frequency factors resulted from the slope and intercept were 31.08 KJ/mol and 6.325×10^4 $(\mathrm{mmol/L})^{-0.3}(\mathrm{gm}_{cat}\ \mathrm{s})^{-1}$ respectively. These values were found to be in agreement with the latest kinetic studies on liquid phase glycerol hydrogenolysis as reported by Vasiliadou and Torres et al. [36,37]. According to Arrhenius law, frequency factor k_o does not affect the temperature sensitivity of the reaction, however in practice, there may be a slight dependency on temperature which is negligible.

4. Conclusions

Co–ZnO catalysts with varying Co and ZnO content were prepared and these catalysts were highly active and selective for hydrogenolysis of glycerol. The activity of the catalysts is dependent on the weight ratio of Co and ZnO and the maximum glycerol hydrogenolysis activity was achieved for the catalyst with Co–ZnO of 50:50 composition by weight. Further, the activity of the catalysts was related to the highly dispersed Co metal area and the amount of ZnO. The process parameters such as reaction temperature, hydrogen pressure, reaction time and glycerol concentration

were optimized to improve the conversion and selectivity of glycerol to 1,2-propanediol. Further, a kinetic model for the glycerol hydrogenolysis reaction with the present catalyst was derived. The proposed Co–ZnO catalyst was stable and can be reusable without any appreciable variation in activity.

Acknowledgement

One of the authors VR thanks CSIR, New Delhi for the award of Senior Research Fellowship.

References

[1] A. Behr, J. Eilting, K. Irawadi, J. Leschinski, F. Lindner, Green Chem. 10 (2008) 13–30.
[2] M. Pagliaro, R. Ciriminna, H. Kimura, M. Rossi, C.D. Pina, Angew. Chem. Int. Ed. 46 (2007) 4434–4440.
[3] Y. Zheng, X. Chen, Y. Shen, Chem. Rev. 108 (2008) 5253–5277.
[4] M.A. Dasari, P.P. Kiatsimkul, W.R. Sutterlin, G.J. Suppes, Appl. Catal. A 281 (2005) 225–231.
[5] J. Chaminand, L. Djakovitch, P. Gallezot, P. Marion, C. Pinel, C. Rosier, Green Chem. 6 (2004) 359–361.
[6] T. Miyazawa, Y. Kusunoki, K. Kunimori, K. Tomishige, J. Catal. 240 (2006) 213–221.
[7] E.P. Maris, R.J. Davis, J. Catal. 249 (2007) 328–337.
[8] M. Balaraju, V. Rekha, B.L.A. Prabhavathi Devi, R.B.N. Prasad, P.S. Sai Prasad, N. Lingaiah, Appl. Catal. A 384 (2010) 107–114.
[9] P. Gallezot, J. Chaminand, L. Djakovitch, P. Marion, P. Catherine, C. Rosier, Green Chem. 6 (2004) 359–361.
[10] I. Gandarias, P.L. Arias, J. Requies, M.B. Güemez, J.L.G. Fierro, Appl. Catal. B 97 (2010) 248–256.
[11] C. Montassier, J.C. Menezo, L.C. Hoang, C. Renaud, J. Barbier, J. Mol. Catal. 70 (1991) 99–110.
[12] B. Casale, A.M. Gomez, US Patent 4, 276, 151, 1994.
[13] C. Montassier, D. Giraud, J. Barbier, Heterogeneous Catalysis and Fine Chemicals, Elsevier Science Publishers, Amsterdam, 1988, pp. 165–170.
[14] M. Tamura, Y. Amada, S. Liu, Z. Yuan, Y. Nakagawa, K. Tomishige, J. Mol. Catal. A: Chem. 388–389 (2014) 177–187.
[15] S. Jin, Z. Xiao, C. Li, C.T. Williams, C. Liang, J. Eng. Chem. 23 (2014) 185–192.
[16] Y. Feng, H. Yin, L. Shen, A. Wang, Y. Shen, T. Jiang, Chem. Eng. Technol. 36 (2013) 73–82.
[17] C. David, D. Françoise, A. Yosslen, S. Philippe, Phys. Chem. Chem. Phys. 13 (2011) 1448–1456.
[18] A. Bienholz, R. Blume, A. Knop-Gericke, F. Girgsdies, M. Behrens, P. Claus, J. Phys. Chem. C 115 (2011) 999–1005.
[19] J. Hu, Y. Fan, Y. Pei, M. Qiao, K. Fan, X. Zhang, B. Zong, ACS Catal. 3 (2013) 2280–2287.
[20] H. Jiye, L. Xiaoyu, F. Yiqiu, X. Songhai, P. Yan, Q. Minghua, F. Kangnian, Z. Xiaoxin, Z. Baoning, Chin. J. Catal. 34 (2013) 1020–1026.
[21] A. Alhanash, E.F. Kozhevnikova, I.V. Kozhevnikov, Catal. Lett. 120 (2008) 307–311.
[22] Y. Kusunoki, T. Miyazawa, K. Kunimori, K. Tomishige, Catal. Commun. 6 (2005) 645–649.
[23] J. Feng, J. Wang, Y. Zhou, H. Fu, H. Chen, X. Li, Chem. Lett. 36 (10) (2007) 1274–1275.
[24] L. Huang, Y.L. Zhu, H.Y. Zheng, Y.W. Li, Z.Y. Zeng, J. Chem. Technol. Biotechnol. 83 (2008) 1670–1675.
[25] X. Guo, Y. Li, R. Shi, Q. Liu, E. Zhan, W. Shen, Appl. Catal. A 371 (2009) 108–113.
[26] M. Balaraju, K. Jagadeeswaraiah, P.S. Sai Prasad, N. Lingaiah, Catal. Sci. Technol. 2 (2012) 1967–1976.
[27] X. Guo, Y. Li, W. Song, W. Shen, Catal. Lett. 141 (2011) 1458–1463.
[28] X. Chu, J. Liu, B. Sun, R. Dai, Y. Pei, M. Qiao, K. Fan, J. Mol. Catal. A: Chem. 335 (2011) 129–135.
[29] C. Tang, C. Wang, S. Chien, Thermochim. Acta 473 (2008) 68–73.
[30] Y. Zhang, D. Wei, S. Hammache, J.G. Goodwin, J. Catal. 188 (1999) 281–290.
[31] N.N. Madikizela-Mnqanqeni, N.J. Coville, J. Mol. Catal. A: Chem. 225 (2005) 137–142.
[32] M. Haneda, Y. Kintaichi, N. Bion, H. Hamada, Appl. Catal. B: Environ. 46 (2003) 473–482.
[33] M. Balaraju, V. Rekha, P.S. Sai Prasad, R.B.N. Prasad, N. Lingaiah, Catal. Lett. 126 (2008) 119–124.
[34] Y. Nakagawa, K. Tomishige, Catal. Sci. Technol. 1 (2011) 179–190.
[35] Y.B. Cao, X. Zhang, J.M. Fan, P. Hu, L.Y. Bai, H.B. Zhang, F.L. Yuan, Y.F. Chen, Crystal Growth Des. 11 (2011) 472–479.
[36] E.S. Vasiliadou, A.A. Lemonidou, Chem. Eng. J. 231 (2013) 103–112.
[37] A. Torres, D. Roy, B. Subramaniam, R.V. Chaudhari, Ind. Eng. Chem. Res. 49 (2010) 10826–10835.